

# SiGe Profile Design Tradeoffs for RF Circuit Applications

Guofu Niu, Shiming Zhang, John D. Cressler, Alvin J. Joseph<sup>1</sup>, John S. Fairbanks<sup>2</sup>, Larry E. Larson<sup>2</sup>, Charles S. Webster<sup>1</sup>, William E. Ansley<sup>3</sup>, and David L. Hareme<sup>1</sup>

Alabama Microelectronics Science and Technology Center, Electrical and Computer Engineering Department, 200 Broun Hall, Auburn University, Auburn, AL 36849, USA

Tel: 334 844-1856 Fax: 334 844-1888 E-mail: guofu@eng.auburn.edu

<sup>1</sup>IBM Microelectronics, Essex Junction, VT 05452, USA

<sup>2</sup>Department of Electrical and Computer Engineering, University of California at San Diego, La Jolla, CA 92093, USA

<sup>3</sup>IBM Microelectronics, Hopewell Junction, NY 12533, USA

*Abstract*— We present the first experimental results for new SiGe profile designs which were developed explicitly for improving minimum noise figure ( $NF_{min}$ ) without sacrificing gain, linearity, frequency response, or the stability of the SiGe strained layer. A measured  $NF_{min}$  of 0.2dB at 2.0GHz with an associated gain ( $G_{assoc}$ ) of 13dB at noise matching, and a linearity efficiency ( $OIP3/P_{DC}$ ) of 10 were obtained for the best low-noise profile, all of which represent substantial improvements in RF performance over the Si BJT and control SiGe HBT design point, and were accomplished without sacrificing SiGe film stability. The fundamental SiGe profile design tradeoffs associated with emerging SiGe RF circuit applications are discussed.

## I. INTRODUCTION

RF applications generally impose more serious device design constraints than digital applications. SiGe HBT technology, because it has higher intrinsic performance than Si BJT technology at similar process complexity, and delivers better cost-performance than GaAs technology, has recently emerged as a contender for the RF market. Existing SiGe profile design points are only optimized for high  $f_T$  and  $f_{max}$  at high current densities [1]. RF transceiver building blocks such as LNA's and mixers, however, often require very low broad band noise, high RF gain, and excellent RF linearity, thus complicating the device design. The fundamental question we address in this paper is the following: given a constraint of maintaining constant film stability, at a given technology generation (i.e., fixed geometry and doping), what is the optimum Ge profile shape that minimizes  $NF_{min}$  without sacrificing gain, linearity, or frequency response? To most efficiently attack the problem, we began with extensive 2-D device simulations using MEDICI [2]. These simulations used 2-D models of the SiGe control profile-based on the device layout and measured SIMS, which were carefully calibrated to data for not only  $\beta$ ,  $f_T$ , and  $f_{max}$ , but also the Y-parameters,  $NF_{min}$ ,

and  $G_{assoc}$ . A new approach [3] [4] for generating all of the noise parameters ( $NF_{min}$ ,  $Y_{opt}$ ,  $R_n$ ) as well as  $G_{assoc}$  from simulated (or measured) Y-parameters was developed for this purpose, and gives excellent agreement with measured noise data.

## II. SiGe PROFILE DESIGN TRADEOFFS

To realize high  $f_T$  and  $f_{max}$  at high  $J_C$  as required by high-speed digital applications, the Ge profile needs to be extended into the neutral collector to minimize the  $f_T$  roll-off at high  $J_C$  due to the high-injection heterojunction barrier effect [5]. LNA's in RF transceivers, however, typically operate at relatively low  $J_C$  where  $NF_{min}$  is minimized (as much as 10x lower in  $J_C$ ). From the theory of linear noisy two-port networks,  $NF_{min}$  is fundamentally determined by the equivalent input current and voltage noise sources [4]:

$$\langle i_n^2 \rangle = 2qI_B + \frac{2qI_C}{|h_{21}|^2} \quad (1)$$

and

$$\langle v_n^2 \rangle = 4kTR_B + \frac{2qI_C}{|y_{21}|^2} \quad (2)$$

where  $y_{21}$  and  $h_{21}$  are the AC transconductance and AC current gain at the frequency of interest, respectively. For a given technology generation (transistor geometries and constant doping), the base resistance  $R_B$  and  $y_{21}$  at a given  $J_C$  are fixed, thus fixing  $\langle v_n^2 \rangle$ .  $\langle i_n^2 \rangle$ , however, can be reduced by increasing  $\beta$  (to reduce  $I_B$ ) and increasing  $f_T$  (to increase  $h_{21}$ ). Consequently  $NF_{min}$  can be reduced. A high  $f_T$  at low  $J_C$  and particularly a high  $\beta$  at low  $J_C$  are therefore critical in reducing  $NF_{min}$  for constant base doping and transistor geometry. From our simulations, we found that for constant film stability (integrated Ge dose), a significant improvement in  $NF_{min}$  over the SiGe control profile can only be realized in practice by pushing the edge of the Ge retrograde in the collector significantly closer to the EB junction (surface), and then using the additional Ge to increase the band offset at the EB junction (for higher

## 22.6.1

$\beta$ ) and increase the Ge grading (for higher  $f_T$ ) [6]. We are thus forced to trade high- $J_C$  performance for improved  $NF_{min}$ . Two such low-noise Ge profiles (LN1 and LN2) which maintain the stability of the SiGe control profile but have significantly lower  $NF_{min}$  in simulation (by 0.2dB) are shown in Fig. 1. All of the SiGe profiles are unconditionally stable to defects generation, as shown in Fig. 2. The two low noise profiles have  $f_{max}$  values comparable to the SiGe control in simulation. The excellent linearity of the Si BJT and SiGe control devices are expected to be retained in the two low noise profiles, because the linearity is primarily determined by the EB and CB depletion capacitances, and insensitive to the diffusion capacitance (base transit time) in this technology [7].

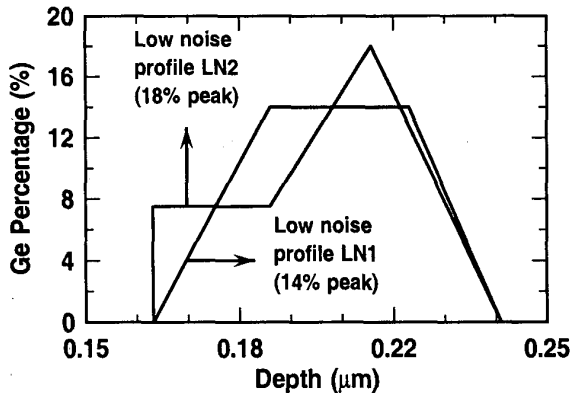


Fig. 1. Schematic of the two low noise profiles designed that are both unconditionally stable.

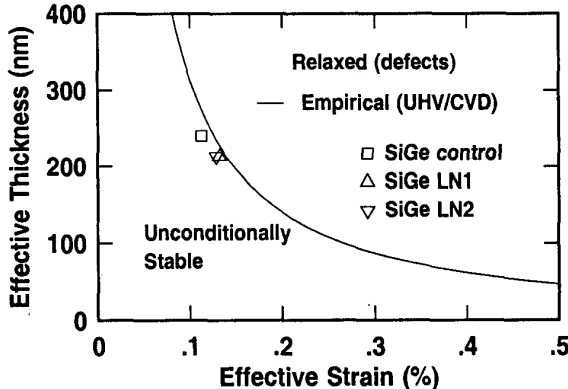


Fig. 2. Stability of the SiGe control design point and the two low noise profiles. All of these profiles are unconditionally stable.

### III. EXPERIMENTAL RESULTS

For unambiguous comparisons all four profiles were fabricated in the same wafer lot in a state-of-the-art  $0.50\mu\text{m}$  SiGe HBT technology [1] using UHV/CVD growth and identical processing conditions. DC characteristics were

TABLE I  
SUMMARY OF DEVICE ELECTRICAL CHARACTERISTICS

Performance	Si BJT	SiGe control	SiGe LN1	SiGe LN2
$\beta$ at $V_{BE}=0.7\text{V}$	67	114	350	261
$V_A$ (V)	19	60	58	113
$BV_{CEO}$ (V)	3.5	3.2	2.7	2.7
$R_{Bi}$ ( $k\Omega/\square$ )	12.8	9.8	10.3	10.7
peak $f_T$ (GHz)	38	52	52	57
peak $f_{max}$ (GHz)	57	64	62	67

measured using an HP4155, and S-parameters were measured using a HP8510C network analyzer from 2 - 40GHz, from which  $f_T$  and  $f_{max}$  were extracted. The noise parameters were measured from 2 - 18GHz using an NP-5 on-wafer measurement system from ATN Microwave Inc., and two-tone load-pull measurements were made at 1.9GHz with 1MHz tone spacing.

Table I summarizes the measured transistor parameters of the four fabricated profiles. The penalty in  $BV_{CEO}$  over the SiGe control for LN1 and LN2 is due to the higher  $\beta$ , and should not impact LNA designs, which see finite source impedance (i.e., not an 'open'). The measured  $\beta_{DC} - I_C$  and  $f_T - I_C$  curves of a  $20\mu\text{m}^2$  ( $0.5 \times 20 \times 2$  stripe) unit cell device are shown in Figs. 3-4, and bear-out the expected high injection design trade-off. The two low noise profiles, LN1 and LN2, have a higher  $\beta_{DC}$  and  $f_T$  at low  $J_C$ , but the SiGe control and Si BJT devices have a weaker (better)  $f_T$  roll-off at high  $J_C$ , as designed. This design tradeoff translates into a significant improvement of the  $NF_{min}$  across the range of  $J_C$  of interest to LNA and mixer circuits over the Si BJT and SiGe control profiles, as shown by the measured  $NF_{min}$  data in Fig. 5. The LN1 profile achieves an impressive  $NF_{min}$  of 0.2dB at 2mA, 0.2dB lower than the SiGe control profile. The measured delta's between profiles are consistent with our simulations. The associated gain at noise matching is still above 13dB at  $NF_{min}$  for all of the profiles ( Fig. 6 ), and the two low noise profiles have  $f_{max}$  comparable to the SiGe control (Fig. 7).

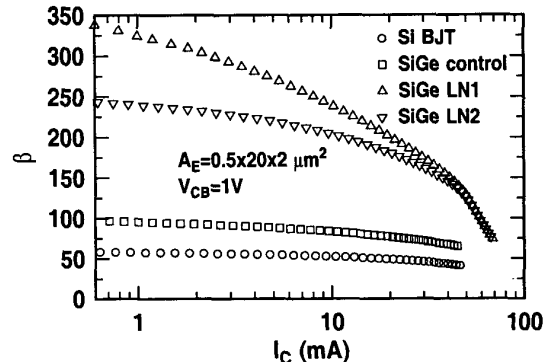


Fig. 3. Measured dc current gain versus collector current of the fabricated Si BJT, SiGe control, and the SiGe low noise profiles.

22.6.2

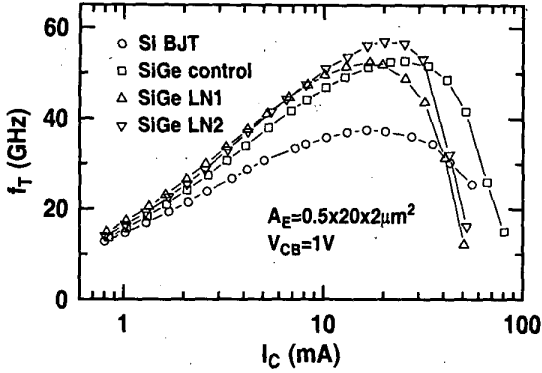


Fig. 4. Measured  $f_T$  versus collector current of the fabricated Si BJT, SiGe control, and the SiGe low noise profiles.

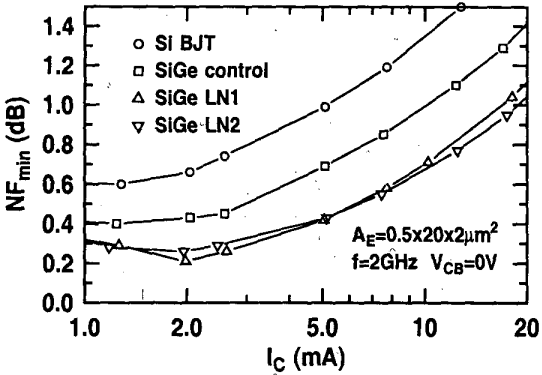


Fig. 5. Measured minimum noise figure ( $NF_{min}$ ) versus collector current at 2GHz for the fabricated Si BJT, SiGe control, and the SiGe low noise profiles.

Two-tone load-pull measurements were performed at 1.9GHz with 1.0MHz tone spacing on the  $20\mu\text{m}^2$  ( $0.5\times 20\times 2$  stripe) unit cell device to determine the linearity. The input 3rd order intermodulation intercept point (IIP3) for a two-tone input is used as a figure-of-merit, and was extracted in the low input power region where the 3rd order intermodulation slope is 3:1. The measured IIP3 is affected by the source and load termination, and thus load-pull data sheds light on the variation of linearity with impedance for each profile. Figs. 8-9 and 10-11 show the measured IIP3 and power gain contours on the load impedance Smith chart for the SiGe control device, and the low noise profile LN1, respectively. The maximum IIP3 achieved is 3dBm (SiGe control) and 3dBm (LN1), with the maximum gain of 17dB (SiGe control) and 20dB (LN1), at 1.9GHz for  $I_C=3\text{mA}$  and  $V_{CE}=3\text{V}$ . An excellent linearity efficiency (defined as  $OIP3/P_{DC}$  to account for the differing load states at maximum gain and maximum IIP3) of 7 and 10 is achieved for the SiGe control and the low noise SiGe profile LN1, respectively, and is comparable to GaAs HEMT (10) and GaAs HBT technology (11) [8]. Preliminary measurements on RF harmonic mixers fabricated with the identical low noise profiles (LN1 and LN2) also show improved noise and linearity over the SiGe control profile, indicating that these device improvements translate to the circuit level.

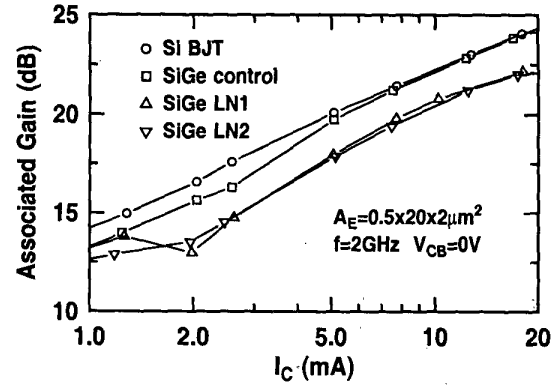


Fig. 6. Measured associated gain versus collector current at 2GHz for the fabricated Si BJT, SiGe control, and the SiGe low noise profiles.

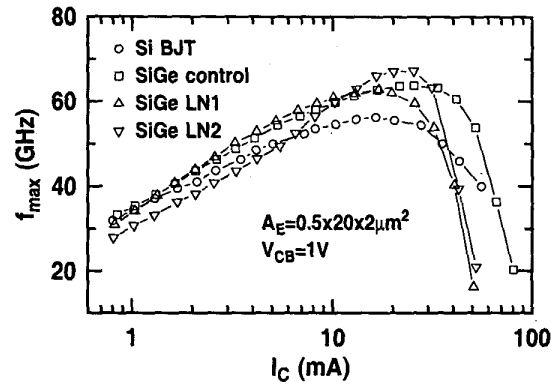


Fig. 7. Measured  $f_{max}$  versus collector current at 2GHz for the fabricated Si BJT, SiGe control, and the SiGe low noise profiles.

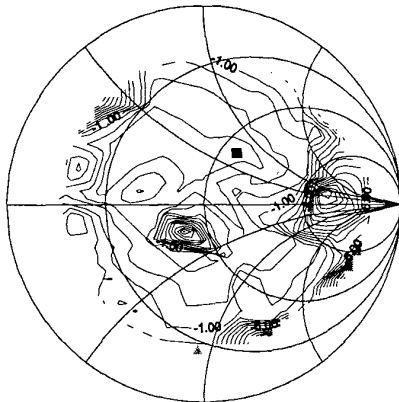
#### IV. CONCLUSIONS

The fundamental SiGe profile design tradeoffs for RF circuit applications have been addressed. A higher DC current gain and a higher  $f_T$  at low  $J_C$  are shown to be critically important for reducing  $NF_{min}$  for a given transistor geometry and doping. By applying careful SiGe profile optimization, significant improvement in RF performance can be achieved. Using a newly developed simulation approach, new SiGe profiles were designed explicitly for improving minimum noise figure ( $NF_{min}$ ) without sacrificing gain, linearity, frequency response, or the stability of the SiGe strained layer. A measured  $NF_{min}$  of 0.2dB at 2.0GHz with an associated gain ( $G_{assoc}$ ) of 13dB at noise matching, and a linearity efficiency ( $OIP3/P_{DC}$ ) of 10 were obtained for the best low-noise profile, all of which represent substantial improvements in RF performance over the Si BJT and control SiGe HBT design point, and were accomplished without sacrificing SiGe film stability.

#### V. ACKNOWLEDGMENTS

The wafers were fabricated at IBM Microelectronics, Essex Junction, VT. We would like to thank D. Ahlgren and B. Meyerson for their contributions to this work.

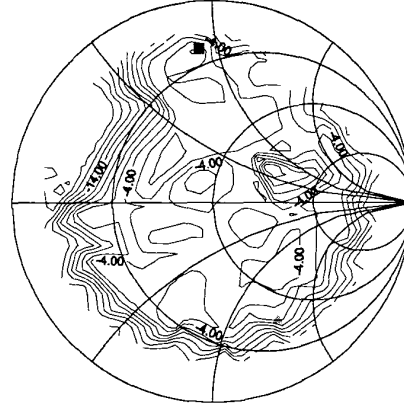
SiGe Control Third-Order Intermodulation Intercept Point  
 $0.5 \times 20 \times 2$ ,  $F=1.9$  GHz,  $I_{ce}=3.0$  mA,  $V_{ce}=3.0$  V



IIP3 Max=2.81 dBm at  $58.9 + j34.9$  load,  
 Source Impedance= $13.9 - j45.8j$  Pin=-24.0dBm

Fig. 8. Measured IIP3 contour on the load impedance Smith chart for the SiGe control device.

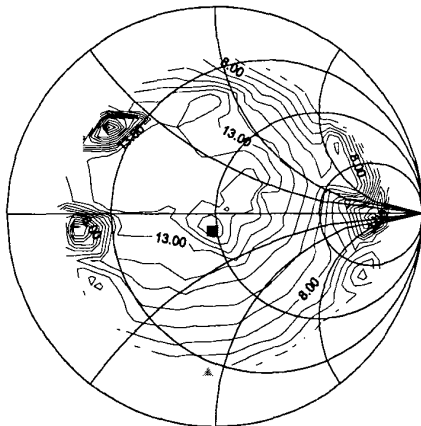
SiGe Low Noise Profile LN1 Third-Order Intermodulation  
 Intercept Point,  $I_{ce}=3.0$  mA,  $V_{ce}=3.0$  V,  $F=1.9$  GHz



IIP3 Max=2.89 dBm at  $11.6 + j44.5$  load,  
 Source Impedance= $33.7 - j73.5j$  Pin=-23.5dBm

Fig. 10. Measured IIP3 contour on the load impedance Smith chart for the low noise profile device LN1.

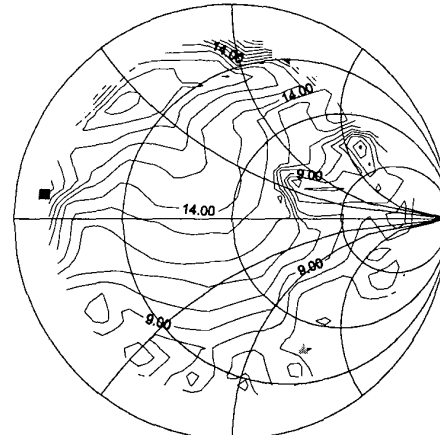
SiGe Control Load-Pull GAIN on  $0.5 \times 20 \times 2$  NPN HBT  
 $I_{ce}=3.0$  mA,  $V_{ce}=3.0$  V,  $F=1.9$  GHz, Pin=-24.0dBm



GAIN Max=17.31 dB at  $48.1 - j8.0$  load  
 Sourc Impedance= $13.9 - j45.8$

Fig. 9. Measured power gain contour on the load impedance Smith chart for the SiGe control device.

SiGe Low Noise Profile LN1 Load-pull GAIN  
 $I_{ce}=3.0$  mA,  $V_{ce}=3.0$  V,  $F=1.9$  GHz,  $0.5 \times 20 \times 2$



GAIN Max=19.82 dB at  $3.6 + j3.3$  load  
 Sourc Impedance= $33.7 - j73.5j$ , Pin=-23.5dBm

Fig. 11. Measured power gain contour on the load impedance Smith chart for the low noise profile device LN1.

#### REFERENCES

- [1] D.C. Ahlgren, M. Gilbert, D. Greenberg, S.J. Jeng, J. Malinowski, D. Nguyen-Ngoc, K. Schonenberg, K. Stein, R. Groves, K. Walter, G. Hueckel, D. Colavito, G. Freeman, D. Sunderland, D.L. Haramé, and B. Beyerson, "Manufacturability demonstration of an integrated SiGe HBT technology for the analog and wireless marketplace," *Tech. Dig. IEDM*, pp. 859-862, 1996.
- [2] MEDICI 4.0, 2-D Semiconductor Device Simulator, *Avant! TCAD*, 1997.
- [3] G.F. Niu, W.E. Ansley, S. Zhang, J.D. Cressler, and R.A. Groves, "A 2-D numerical simulation methodology for noise figure optimization in UHV/CVD SiGe HBT's," *Tech. Dig. IEEE Symposium on Monolithic Integrated Circuits in RF Systems*, pp. 253-257, 1998.
- [4] G.F. Niu, W.E. Ansley, S. Zhang, J.D. Cressler, C.S. Webster, and R.A. Groves, "Noise parameter optimization of UHV/CVD SiGe HBT's for RF and microwave applications," *IEEE Trans. Electron Devices*, vol. 46, no. 8, pp. 1347-1354, August 1999.
- [5] A.J. Joseph, J.D. Cressler, D.M. Richey, and D.L. Haramé, "Impact of profile shape on the high injection barrier effects in advanced UHV/CVD SiGe HBT's," *Tech. Digest. IEDM*, pp. 253-256, 1996.
- [6] W.E. Ansley, J.D. Cressler, and D.M. Richey, "Base profile optimization for minimum noise figure in advanced UHV/CVD SiGe HBT," *IEEE Trans. Microwave Theory and Techniques*, vol. 46, no. 5, pp. 653-660, May 1998.
- [7] G.F. Niu, J.D. Cressler, W.E. Ansley, C.S. Webster, R. Anna, and N. King, "Intermodulation characteristics of UHV/CVD SiGe HBT's," to appear in *Proc. IEEE BCTM*, September 1999.
- [8] N. King and A. Victor, "Enhanced wireless circuit performance with SiGe technology," *IBM MicroNews*, 1st quarter, pp. 5-10, 1999.